

# Vapour pressure deficit was not a primary limiting factor for gas exchange in an irrigated, mature dryland Aleppo pine forest

Yakir Preisler<sup>1,2</sup>  | José M. Grünzweig<sup>2</sup> | Ori Ahiman<sup>2,3</sup> | Madi Amer<sup>1</sup> | Itai Oz<sup>1,2</sup> | Xue Feng<sup>4</sup>  | Jonathan D. Muller<sup>1,5</sup>  | Nadine Ruehr<sup>6</sup> | Eyal Rotenberg<sup>1</sup> | Benjamin Birami<sup>6</sup> | Dan Yakir<sup>1</sup>

<sup>1</sup>Department of Earth and Planetary Science, Weizmann Institute of Science, Rehovot, Israel

<sup>2</sup>Robert H. Smith Faculty of Agriculture, Food and Environment, The Hebrew University of Jerusalem, Rehovot, Israel

<sup>3</sup>Institute of Soil, Water and Environmental Sciences, ARO Volcani Center, Beit Dagan, Israel

<sup>4</sup>Department of Civil, Environmental, and Geo-Engineering, University of Minnesota, Minneapolis, Minnesota, USA

<sup>5</sup>School for Climate Studies, Stellenbosch University, Stellenbosch, South Africa

<sup>6</sup>Institute of Meteorology and Climate Research-Atmospheric Environmental Research (IMK-IFU), KIT-Campus Alpin, Karlsruhe Institute of Technology (KIT), Garmisch-Partenkirchen, Germany

## Correspondence

Yakir Preisler, Department of Organismic and Evolutionary Biology, Harvard University, 16 Divinity Av. Cambridge MA. USA 02138.  
Email: [ypreisler@fas.harvard.edu](mailto:ypreisler@fas.harvard.edu)

## Present address

Yakir Preisler, Department of Organismic and Evolutionary Biology, Harvard University, Cambridge, Massachusetts, USA.

## Funding information

German Research Foundation, Grant/Award Numbers: YA 274/1-1, SCHM 2736/2-1; Israel Science Foundation, Grant/Award Number: ISF 1976/17; NSFC-ISF, Grant/Award Number: 2579/16; Keren Kayemet Lelsrael, Grant/Award Number: KKL 90-10-012-11; Ring Family Foundation; United States-Israel Binational Agriculture Research and Development Fund, Grant/Award Number: FI-584-2019; National Science Foundation, Grant/Award Number: DEB-2045610

## Abstract

Climate change is often associated with increasing vapour pressure deficit (VPD) and changes in soil moisture (SM). While atmospheric and soil drying often co-occur, their differential effects on plant functioning and productivity remain uncertain. We investigated the divergent effects and underlying mechanisms of soil and atmospheric drought based on continuous, in situ measurements of branch gas exchange with automated chambers in a mature semiarid Aleppo pine forest. We investigated the response of control trees exposed to combined soil-atmospheric drought (low SM, high VPD) during the rainless Mediterranean summer and that of trees experimentally unconstrained by soil dryness (high SM; using supplementary dry season water supply) but subjected to atmospheric drought (high VPD). During the seasonal dry period, branch conductance ( $g_{br}$ ), transpiration rate ( $E$ ) and net photosynthesis ( $A_{net}$ ) decreased in low-SM trees but greatly increased in high-SM trees. The response of  $E$  and  $g_{br}$  to the massive rise in VPD (to 7 kPa) was negative in low-SM trees and positive in high-SM trees. These observations were consistent with predictions based on a simple plant hydraulic model showing the importance of plant water potential in the  $g_{br}$  and  $E$  response to VPD. These results demonstrate that avoiding drought on the supply side (SM) and relying on plant

**Abbreviations:**  $A_{net}$ , branch chambers Net photosynthesis  $\mu\text{mol m}^{-2} \text{s}^{-1}$ ;  $E$ , branch chambers transpiration  $\text{mmol m}^{-2} \text{s}^{-1}$ ;  $g_{br}$ , branch chambers stomatal conductance  $\text{mol m}^{-2} \text{s}^{-1}$ ;  $g_s$ , stomatal conductance  $\text{mol or mmol m}^{-2} \text{s}^{-1}$ ; LSA, leaf specific area  $\text{m}^{-2}$ ; PET, potential evapotranspiration  $\text{mm yr}^{-1}$ ; REW, relative extractable water unitless; SF, sap flow liter  $\text{h}^{-1} \text{tree}^{-1}$ ; SM, soil moisture %; VPD, vapour pressure deficit kPa;  $\Psi_{leaf}$ , leaf water potential MPa;  $\Psi_{soil}$ , soil water potential MPa.

This is an open access article under the terms of the Creative Commons Attribution-NonCommercial License, which permits use, distribution and reproduction in any medium, provided the original work is properly cited and is not used for commercial purposes.

© 2023 The Authors. *Plant, Cell & Environment* published by John Wiley & Sons Ltd.

hydraulic regulation constrains the effects of atmospheric drought (VPD) as a stressor on canopy gas exchange in mature pine trees under field conditions.

#### KEYWORDS

automated branch chambers, drought, irrigation, semiarid, soil moisture, supply and demand, transpiration, VPD, water potential

## 1 | INTRODUCTION

Recent years have seen water scarcity and rising temperatures in a range of ecosystems, which have contributed to an alarming increase in reports of large-scale drought-related tree mortality in various biomes (Allen et al., 2010, 2015; Cobb et al., 2017; Hammond et al., 2022; Hartmann et al., 2022; Preisler et al., 2019). The response of forest trees to water stress in semiarid lands is critical both for predicting future land cover changes in these regions and for any attempt to minimise its effects through management (Alpert et al., 2008; Burke et al., 2006; IPCC, 2018). Studying the response of trees to ecological drought remains challenging for two main reasons. First, because water stress can be driven by either lower precipitation and soil moisture (SM) content or increased atmospheric evaporative demand, such interactions are not well resolved at present in ecophysiological and Earth system models (Anderegg et al., 2018; Bartlett et al., 2018; Dracup et al., 1980; Lloyd-Hughes, 2014; Mirfenderesgi et al., 2016; Sperry & Love, 2015; Sperry et al., 2016; Tate & Gustard, 2000). Second, while control experiments in the laboratory or growth chamber (e.g., Grossiord et al., 2017) can help resolve the contribution to water stress, this is seldom achieved under field conditions in mature trees, which is critical for validating control experiments and making realistic predictions. Furthermore, previous reports of stomatal response to variations in SM and vapour pressure deficit (VPD) tended to focus on temperate environments with relatively high SM and low VPD and a limited range of variability, even in dry conditions (Novick et al., 2016; Hochberg et al., 2017; Domec et al., 2009; Grossiord et al., 2017; Maseyk et al., 2008; Ruehr et al., 2012). Therefore, the environmental factors and use of mature trees under field conditions extend the range of habitats and conditions and improve the understanding of how trees will respond to drier conditions that may apply to the Mediterranean and possibly other mesic environments undergoing climate change.

Climatic models predict that drought severity and temperature rises will further intensify in the coming decades (Alpert et al., 2008; Burke et al., 2006; IPCC, 2018). Ecological drought is commonly described as a period characterised by water deficit owing to lower than average precipitation and/or increased air temperatures and leading to higher evaporative demand of the atmosphere (Dracup et al., 1980; Lloyd-Hughes, 2014; Tate & Gustard, 2000). Droughts are commonly classified into two types, namely, soil drought and atmospheric drought, which are associated with water deficits in soil and the occurrence of a relatively VPD in the air, respectively. High VPD values occur during the dry season and are often accompanied

by soil drought. Nevertheless, exceptions to the coupling of atmospheric and soil droughts can occur, for example, in irrigated agricultural fields, desert riparian zones, and groundwater-fed forests. Research addressing the effects of global warming tends to focus on the role of temperature (Park Williams et al., 2013) and often neglects the fact that VPD will increase at a faster rate than temperature (Breshears et al., 2013). Furthermore, there is currently an increasing number of studies that ask whether soil or atmospheric drought independently dominates plant function and drought stress over the other factor, with an increasing focus on the effects of VPD. Recent studies, particularly over large spatial scales, show that either SM, VPD, or their combined effects dominate stomatal conductance, carbon uptake, and modelled plant water stress responses (Novick et al., 2016; Feldman et al., 2020; Stocker et al., 2018; L. Liu et al., 2020; Y. Liu et al., 2020; Rigden et al., 2020). Additionally, the certainty in the predicted changes in SM is low (Ault, 2020; IPCC, 2018, 2021). These considerations make the question of plant responses to atmospheric versus soil drought a matter of particular importance in high-VPD environments, especially when soil water supply and atmospheric moisture demand act as independent drivers of transpiration.

VPD is traditionally linked to decrease in stomatal conductance, preventing excessive water loss via transpiration (Damour et al., 2010; Lange et al., 1971; Novick et al., 2016; Oren et al., 1999). Plants regulate water loss via stomatal closure to maintain hydraulic safety and to balance their water supply with atmospheric moisture demand (Choat et al., 2012; Sperry, 2000). Stomatal closure dynamically decreases transpiration in response to soil drought and increased VPD (due to temperature rises and/or reduction in air humidity) (Ball et al., 1987; Buckley, 2005; Cochard et al., 1996; Meinzer et al., 2009; Tyree & Sperry, 1988; Woodruff et al., 2008). The physical and chemical mechanisms through which stomatal closure occurs involve leaf turgor loss, osmotic regulation, ion pumps and abscisic acid production (Brodribb et al., 2003; Haworth et al., 2011; McAdam & Brodribb, 2012, 2014), all of which are governed by leaf water potential ( $\Psi_{\text{leaf}}$ ), which regulates guard cell activity (Anderegg et al., 2018; Brodribb & Holbrook, 2003; Cochard et al., 1996; Jarvis, 1976; Wolf et al., 2016). While some physiological and Earth system models have started to incorporate  $\Psi_{\text{leaf}}$  and plant hydraulic status as a controlling factor of stomatal conductance ( $g_s$ ) (Anderegg et al., 2018; Dewar et al., 2018; Sperry & Love, 2015; Wolf et al., 2016), the majority still use empirical equations to simulate stomatal regulation as a function of its external environmental drivers, such as VPD (e.g., Damour et al., 2010; Medlyn et al., 2017;

Oren et al., 1999). Modelling stomatal closure as a direct result of VPD may miss important physiological adjustments in cases where SM is decoupled from VPD. Thus, studies intending to disentangle the effects of SM and VPD on transpiration have revealed that VPD seemingly exerts more influence than SM on stomatal closure (Damour et al., 2010; Novick et al., 2016), indicating a direct link between increased VPD and reduced  $g_s$ . However, studies on pine trees revealed that under semiarid conditions (mean annual rainfall of 415 mm), the main limiting factor of gas exchange was SM and not VPD (Grossiord et al., 2017) and that stomatal conductance sensitivity to VPD was governed by SM (Ruehr et al., 2012). Domec et al. (2009) found that in moist sites with apparently sufficient water supply (annual rainfall >1200 mm), the main limiting factor for tree transpiration shifted from VPD to SM as the soils became drier. A similar dominant effect of SM on transpiration was also shown in drier sites (Maseyk et al., 2008). These findings may have resulted from SM and VPD being correlated in these studies and from the fact that when SM was high, VPD did not exceed 3.5 kPa.

Separating the responses of trees to soil and atmospheric drought under field conditions is challenging. Nevertheless, the contradictory indications noted above highlight the urgent need to assess the relative effects of SM and VPD to more accurately predict tree responses to extreme drought under natural conditions (Park-Feldman et al., 2020; Novick et al., 2016; Park Williams et al., 2013; L. Liu et al., 2020). Here, we addressed this challenge by (1) taking advantage of the large seasonal increase in VPD in a semiarid pine forest during the dry season (Wang et al., 2020) and (2) eliminating seasonal soil drought by supplementing irrigation during the high VPD period. A system of automated branch chambers allowed for continuous tree gas exchange monitoring in both low-SM control and high-SM irrigated trees over the full annual cycle, providing an opportunity to characterise the trees' physiological response in situ.

## 2 | MATERIALS AND METHODS

### 2.1 | Study site and experimental design

The study was carried out in the FLUXNET site of Yatir forest (Grünzweig et al., 2003; Rotenberg & Yakir, 2010), a semi-arid, 55-year-old forest planted predominantly with Aleppo pine (*Pinus halepensis* Mill.), located in the northern edge of the Negev desert, Israel (31° 20' 42"N 35° 3' 7.2"E, 550–700m a.s.l.). The climate is Mediterranean with prolonged summer drought periods with no rainfall from May to October (average daily temperature in July is 25°C) and a winter period with low precipitation ( $P = 279 \pm 90$ ; 1970–2018 mean) and moderate temperatures (~10°C in January). Potential evapotranspiration (PET) averaged 1600 mm yr<sup>-1</sup> and P/PET averaged 0.17. During the dry season, the maximum VPD value reached 6.5 kPa and the SM minimum reached 5%–10 % at 10–40 cm depth (multiannual values; 2001–2020).

Two adjacent study areas were established near the flux tower site (yet not affecting its footprint): one serving as an ambient control (Low SM) and the other functioning as an irrigated area (High SM). These areas were separated by a 30-m wide buffer strip and had similar characteristics (aspect, slope, tree density and age, soil depth, etc.), each consisting of 30 trees (with a mean height and diameter of 12 and 18 cm, respectively), and covering an area of 1000 m<sup>-2</sup>. Tree sap flow (SF) was continuously measured since 2015 in 40 trees (17 in each plot of Low SM and High SM treatments, and six in the buffer area), by lab-made heat dissipation sensors (Granier, 1985). For a detailed explanation of the SF and site-specific methodology, see Klein et al. (2014) and Cohen et al., (2008).

### 2.2 | Soil moisture (SM)

SM (%) was monitored in the study plots from August 2016 to date, using five access tubes per area, with specific calibration curves for each access tube (PR2/6, Delta T Devices) to a depth of 100 cm (10, 20, 40, 60, and 100 cm), (Supporting Information: Figure S1). To obtain a relative index of the SM, which was available to the main root systems of the trees (10–60 cm depth), as demonstrated by Preisler et al. (2019), the SM was scaled according to its minimum (11%) and field capacity (42%) values, expressed as relative extractable water (REW), as described by Granier et al. (1999, 1987). Hence REW = 0 at SM of 11% and REW = 1 at SM of 42% mean values of 0–60 cm.

### 2.3 | Branch chambers

To enable the continuous measurements of photosynthesis and transpiration in the harsh field conditions, custom-made branch chambers were designed, modified from Bamberger et al. (2017) and Pumpanen et al. (2009). The experimental setup included 16 in situ branch chambers installed at a mid-canopy height of 6 m (Supporting Information: Figure S1). Each of the seven chambers per treatment housed an intact branch attached to the tree, while one empty chamber served as a background reference air to examine the chamber effect (blank). Each chamber contained a branch with four twigs, which was replaced every month to ensure representative measurements of the whole tree. The azimuth of the monitored branch on a tree was randomly selected, to represent all parts of the mid-canopy heterogeneity. The chambers remained open, except during the short periods when the measurements were taken (4 min h<sup>-1</sup> randomized between chambers) when a movable lid automatically closed. A programmed magnetic valve controlled the randomized air sampling from the chambers (for more details, see Supporting Information: Figure S2). The chambers were constructed from a transparent cylinder enclosed by two caps (inner volume: 11.2 L), all made of highly light-transmitting Perspex. The chamber material resulted in some attenuation of the incident light, but the large range of photosynthetic photon flux density (PPFD) values

observed at the study site did not prevent the comparison between treatments (see Muller et al., 2021b for details).

The accurate measures of the  $H_2O$  and  $CO_2$  fluxes were performed using a setup that consisted of two infrared gas analyzers (IRGAs): one for absolute ambient values was used as a reference air (LI-840A; LI-COR) situated in-between the two plots at 6 m height,

and the other for differential measurement (LI-7000), randomly sampled from each chamber over 4 min (Figure 1 and Supporting Information: Figure S2). The LI-7000 IRGA measured the differences in water vapour and the  $CO_2$  levels between the ambient air (as obtained from the LI-840A) and the sample air coming from each chamber. Using a local ambient gaseous concentration in the LI840A

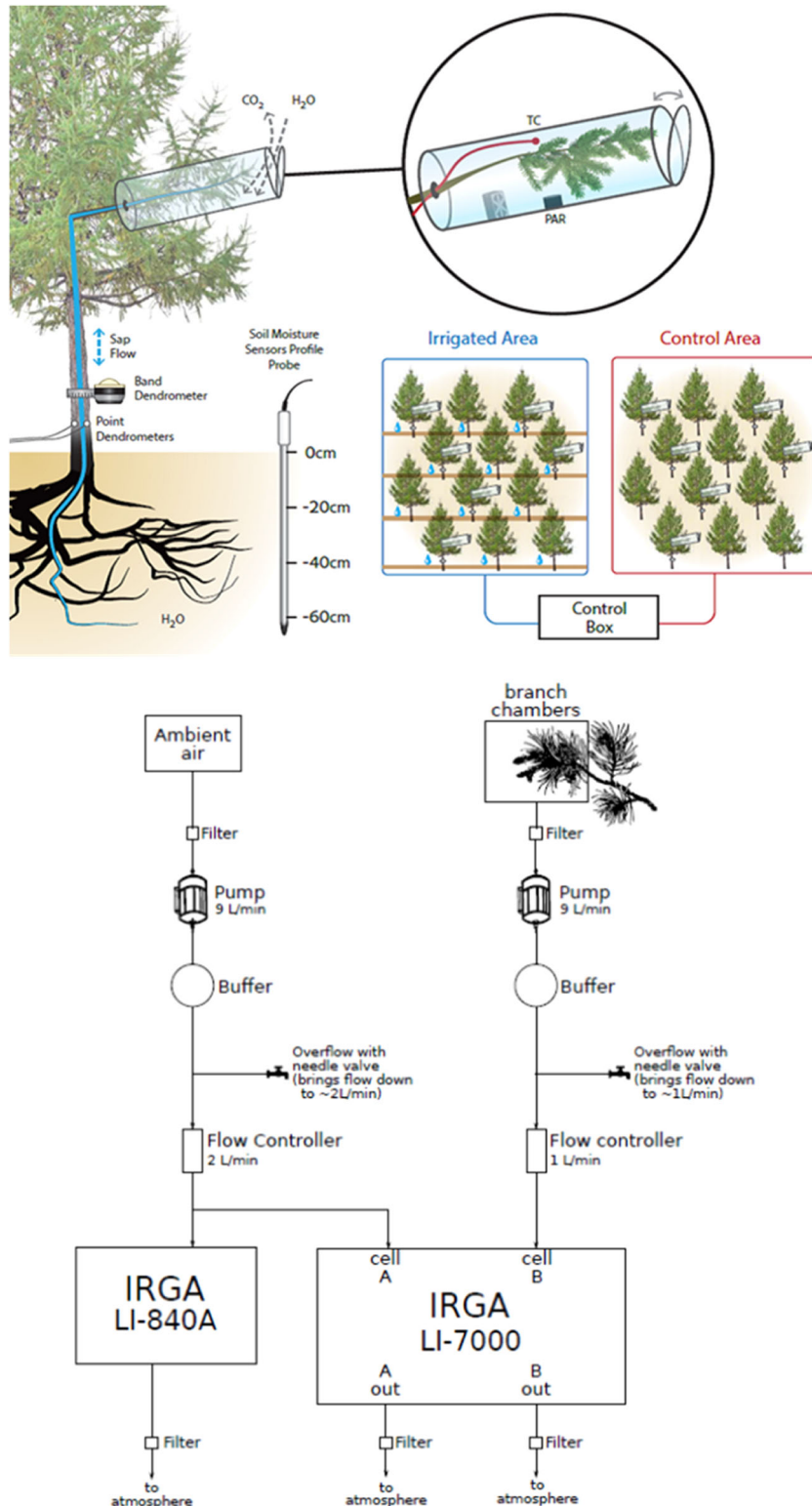


**FIGURE 1** Diagrams of the gas exchange measurement setup (bottom) and illustration of the sensor installation and plot design in the study area (top). For simplification, the measurement principle is represented by two chambers. The field setup consisted of 14 branched chambers and two empty chambers, measured in sequence. The chambers remained open except for short periods of 4 min per hour, when the measurements were taken, and a movable lid automatically closed the chamber. The direction of airflow is indicated by the small arrows. Dendrometer data are not shown, and sap flow data are shown in the supplementary information (Supporting Information: Figure S4). [Color figure can be viewed at [wileyonlinelibrary.com](https://onlinelibrary.wiley.com/doi/10.1111/pcel.14712)]

IRGA allowed us to obtain absolute  $H_2O$  and  $CO_2$  values at the resolution and accuracy needed to calculate expectedly low rates of transpiration and photosynthesis. VPD values were obtained from ambient temperature and  $H_2O$  concentrations inside each chamber.

A photosynthetic photon flux density (PPFD) sensor (calibrated g1118 photodiode; Hamamatsu Photonics K. K.) and a self-made type T (Copper/Constantan) fine thermocouple (REOTEMP Instrument Corporation) were located in the center of each chamber. A small 12 V electronic fan (JAMICON) continuously circulated air inside the chamber to ensure homogeneous air mixing.

## 2.4 | Calculation of fluxes

Projected leaf area (LA) was estimated every month for each chamber separately without destructive sampling inside the chamber. This was done by measuring the current twigs LA and replacing them with other new twigs monthly. For detailed description of LA estimation see (Oz, 2021).

$H_2O$  ( $mmol\ m^{-2}\ s^{-1}$ ) and  $CO_2$  ( $\mu mol\ m^{-2}\ s^{-1}$ ) fluxes, that is, transpiration ( $E$ ) and photosynthesis ( $A_{net}$ ), were calculated using the differences in the  $H_2O$  and  $CO_2$  concentrations between the sample chambers and the empty reference chamber, the measured flow rate, and the heat capacity and density of moist air (calculated from air pressure). The calculations were performed using the following equations (von Caemmerer & Farquhar, 1981):

$$E = \frac{f\Delta H_2O}{LSA}, \quad (1)$$

$$A_{net} = \frac{f\Delta CO_2}{LSA} - C_s E, \quad (2)$$

where  $\Delta H_2O$  ( $mmol\ mol^{-1}$ ) and  $\Delta CO_2$  ( $\mu mol\ mol^{-1}$ ) are the differences in the concentrations between the ambient (outside air) and sample (from a branch chamber) air;  $f$  denotes the flow rate through the chamber, expressed as the volume of air in moles ( $mol/s$ ), that passes through the chamber per second and  $LSA$  is leaf specific area;  $A_{net}$  is corrected for the dilution via the outgoing transpiration fraction ( $C_s E$ ); and  $C_s$  is the ambient  $CO_2$  concentration. The scripts used to calculate all the data, including example data are available online <https://github.com/kebasaa/Branch-chamber-fluxes> (Muller & Oz, 2021).

It was not possible to determine the accurate temperature of each of the approximately 100–150 needles inside a chamber. Thus, we used air temperature ( $T_a$ ), measured by the thermocouple that was located among the needles, to calculate the leaf-to-air VPD. Branch conductance ( $g_{br}$  in  $mol\ m^{-2}\ s^{-1}$ ) was then computed as follows:

$$g_{br} = \frac{E \left( 1000 - \frac{e_l + H_2O_{out}}{2} \right)}{e_l - H_2O_{out}}, \quad (3)$$

where  $e_l$  stands for the mole fraction of leaf vapor pressure (assuming saturation in the sub-stomatal cavity [Gaastra, 1959] using Equation 3)

and  $H_2O_{out}$  is the water concentration in the ambient air plus the  $H_2O$  molecules added by transpiration, resulting in leaf-to-air VPD.

$$e_l = 0.61365 e^{\left( \frac{17.592 T_l}{240.97 + T_l} \right)} \quad (4)$$

$T_l$  is estimated near-leaf temperature in  $^{\circ}C$ .

## 2.5 | Irrigation treatment

To control SM, we employed five soil moisture sensors at average depths of 20–60 cm ( $n = 5$  probes at each depth, every 10 cm) in the High SM plot to operate as ON/OFF switches for the irrigation system. The threshold ranged between 0.6 and 0.7 REW (equivalent to 30%–33% SM) as the mean value of the five sensors. This range was maintained throughout the study period. Drip irrigation provided water at a rate of  $1.6\ L\ h^{-1}$  to an area of  $30 \times 35\ m$  ( $1050\ m^2$ ), with 1 m lateral spacing between the lines and 30 cm dripper spacing. On the 14 May 2017, the irrigation was initiated at a time when the mean REW was 0.3 (SM = 19%) (Figure 2). Note that the drip irrigation was used on a small plot of 0.1 ha, in a large forest (~2500 ha) of low density—high turbulence with minimal environmental effects, and therefore no environmental effect, as was also reported in our preceding paper (Muller et al., 2021).

## 2.6 | Two seasonal peak periods

To identify the impact of eliminating summer soil drought on the trees' activities across the seasonal cycle, we used the long-term measurement dataset of the Yatir forest flux tower data to compare the peak activities at the tree and ecosystem scales. At the ecosystem scale, the peak activity was identified (see Maseyk et al., 2008; Rotenberg & Yakir, 2011; Wang et al., 2020) in March during the wet season, with mean midday VPD =  $1.43 \pm 0.04\ kPa$ , and the lowest activity occurred in July, during the maximum annual mean midday VPD three times higher than March ( $4.46 \pm 0.12\ kPa$ ). A comparison between these two seasons is held to evaluate the response to irrigation.

## 2.7 | Model description and equation

To elucidate the soil and atmospheric drivers of tree transpiration, we used a mathematical model (modified from Feng et al., 2018) to describe the relationships between  $E$ ,  $g_{br}$ ,  $\Psi_s$ , and VPD. The model couples a canopy conductance model with a plant hydraulics model along the soil–plant–atmosphere continuum. To simplify the model, it is applicable at the daily scale under assumptions of equilibrated, daily averaged transpiration rates and negligible water storage in the plant. Water potential is expressed in the model as the daytime average, nighttime fluxes are assumed to be negligible, and gravitational effects are disregarded.

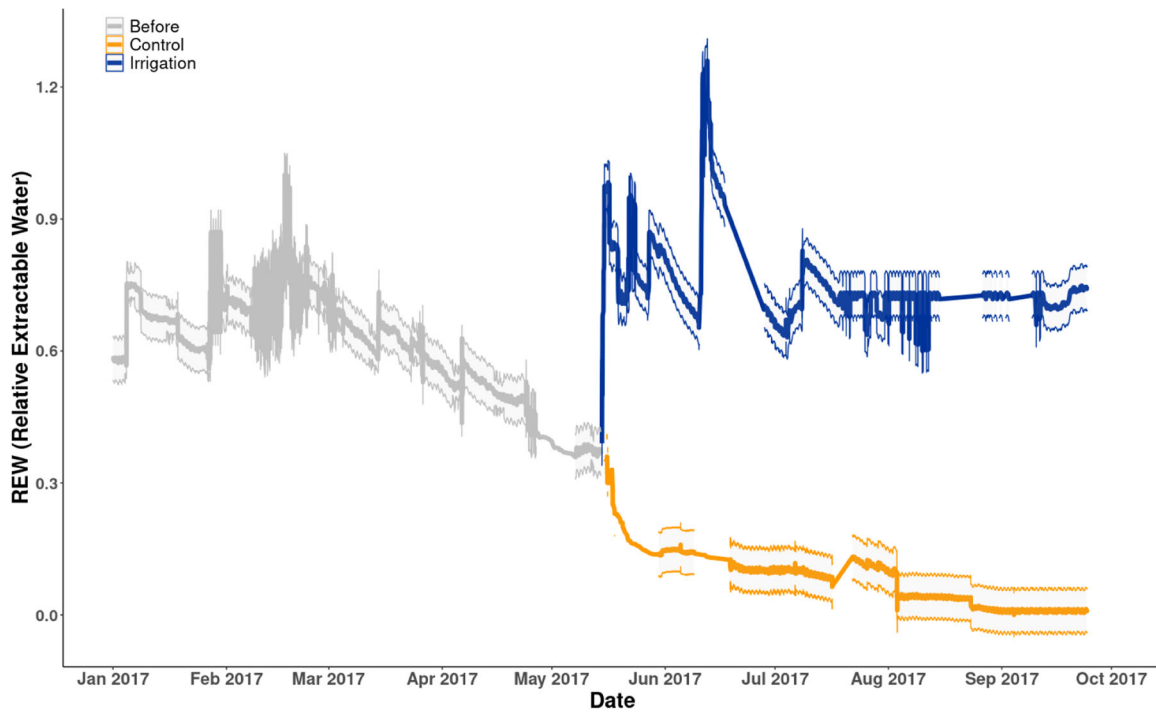


**FIGURE 2** Annual trend of relative extractable water (REW) measured at the main root zone (10–60 cm) before (gray line,  $n = 4$  sensors each plot) and after the onset of irrigation in the high-soil moisture (SM) (blue line;  $n = 5$ ), and low-SM (orange line;  $n = 5$ ) plots. Irrigation began on May 14, 2017 (green dashed line). Missing data are due to sensor transition or malfunction. [Color figure can be viewed at [wileyonlinelibrary.com](http://wileyonlinelibrary.com)]

Branch-level stomatal conductance ( $\text{mmol m}^{-2} \text{s}^{-1}$ ) is described as follows:

$$g_{br} = g_{s,\max} \frac{1}{\exp\left[\left(-\frac{\psi_p}{\beta}\right)^\beta\right]}, \quad (5)$$

where  $g_{s,\max}$  is a parameter for maximum stomatal conductance and  $\beta$  is the sensitivity of the stomatal conductance to the plant water potential,  $\psi_p$ . The daily branch-level transpiration flux ( $\text{mmol m}^{-2} \text{s}^{-1}$ ) is given by:

$$E = g_{br}(\psi_p) \cdot D \cdot L, \quad (6)$$

in which  $D$  represent the daytime-averaged VPD ( $\text{mol H}_2\text{O mol}^{-1} \text{air}$ ) and  $L$  is the leaf area per sapwood area. Transpiration supply is regulated by the hydraulic potential gradient from the soil to the canopy, along with hydraulic resistances along the SPAC. Such resistances are modeled as continuous resistances; a matrix flux potential  $\Phi$  serves to drive the flow and is derived by integrating a hydraulic conductance,  $k$ , across gradients of water potential  $\psi$  (i.e.,  $\Phi = \int_{-\infty}^{\psi_p} k(\psi) d\psi$ ), using the Kirchhoff transformation (Ross & Bristow, 1990; Sperry et al., 1998). The daily transpiration water flux from the soil to the canopy is therefore expressed as follows:

$$E = - \int_{\psi_s}^{\psi_p} k_X(\psi) d\psi = -(\Phi_p - \Phi_s), \quad (7)$$

where  $\psi_s$  and  $\psi_p$  are the water potential values in the soil and plant (MPa), and  $k_X$  is the stem conductance ( $\text{m}^3 \text{d}^{-1} \text{MPa}^{-1}$ ), described as a function of the declining plant water potential, as determined using the exponential sigmoidal function (Pammenter & Willigen, 1998):

$$k_X(\psi_p) = k_{X,\max} \left( 1 - \frac{1}{1 + e^{a(\psi_p - \psi_{X50})}} \right), \quad (8)$$

where  $\psi_{X50}$  is the water potential at a 50% loss, relative to the maximum stem conductivity  $k_{X,\max}$ , and  $a$  denotes a fitting parameter for the stem vulnerability curve.

Simultaneously solving Equations (6) and (7) yields the solution to  $(E, \gamma_p)$  given inputs for soil water potential  $\psi_s$  and vapour pressure deficit  $D$ . To calibrate the model, the measurements of daily average transpiration rate from *P. halepensis* and VPD were used in combination with the following assumed parameters:  $a = 1$ ,  $\beta = 1$ , and  $\gamma_{X50} = -3.5$  MPa (Oliveras et al., 2003; Klein et al., 2011; David-Schwartz et al., 2016). Additionally, the  $\Psi_s$  values of the High SM individuals were assumed to be constant at  $\psi_s = -0.5$  MPa (mean  $\Psi_s$  was determined using the [Saxton et al., 1986] model with measured SM), and the  $\Psi_s$  values of the Low SM individuals were assumed to decrease incrementally with a simulated increase in VPD from  $\gamma_{s,0}$  to  $\gamma_{s,\min}$ . Three fitting parameters were employed to calibrate the model against the daily averaged branch-level stomatal conductance data: the maximum stomatal conductance ( $g_{s,\max}$ ) and the maximum and minimum  $\Psi_{\text{soil}}$  values under the control settings

( $y_{S,0}$  and  $y_{S,\min}$ , respectively). The fitted values were then used to predict daily branch-level transpiration fluxes during the wet and dry seasons, for both High SM and Low SM individual trees.

## 2.8 | Data and statistical analysis

Chamber data ( $E$ ,  $g_{br}$ , and  $A_{net}$ ) were expressed as the average values of the seven chambers per plot, with the standard error shown in the error bars for each plot. As all the chambers were sampled at random time points every hour, we obtained a decent representation of each area per hour for all days, and each value derived from each area was labelled as corresponding to the trees located in either the Low SMA or High SM plots. Data analysis and calculations were performed using MATLAB R2016b (MathWorks). Analysis of variance and Student  $t$ -tests were routinely applied to determine the significance of the differences between the treatments while accounting for the repeated measures of the same chambers. When normality tests failed, the Whitney–Mann sum rank test was used.

## 3 | RESULTS

### 3.1 | Pretreatment comparison

Using the permanently installed branch chamber system (Figure 1), we assessed branch gas exchange before irrigation (January–May 2017) when SM in both treatment plots was similar ( $p = 0.14$ ; Figure 2), and we

found no differences between the treatments in tree activity (all  $p$  values  $> 0.05$ ), as expressed in sap flow ( $p = 0.43$ ; Supporting Information: Figure S4),  $E$  ( $p = 0.13$ ),  $A_{net}$  ( $p = 0.31$ ), or  $g_{br}$  ( $p = 0.15$ ) (Figure 3a–c). During April 2017, branch conductance was higher in the high-SM plot before the onset of irrigation for no apparent reason, which likely reflected natural variations among the chamber measurements under the field conditions and the amount of available data at each plot (see Supporting Information: Figure S3). The VPD values inside the branch chambers did not differ between plots before the onset of irrigation but were slightly lower ( $p > 0.05$ ) in the high-SM chambers after the start of irrigation due to higher chamber humidity caused by higher transpiration rates (Figure 4; Supporting Information: Figure S5). Notably, although there was a minor difference in mean VPD values between chambers when the lid was briefly closed for measurement (4 min), the comparative nature of the experimental plots was unaffected thanks to a large number of measurements ( $n > 1000$ ) encompassing a large range of VPD values, including the high-end values.

### 3.2 | Initial response to supplemental irrigation during the dry season

The relative extractable water from the soil root zone (REW) increased from 0.29 to 0.71 immediately (2–3 days) after irrigation started (Figure 2) and remained high at  $0.68 \pm 0.005$  (mean  $\pm$  SE) during the entire study period. In contrast, the low-SM plot gradually dried out, with REW decreasing from 0.30 to 0.06 by the end of the dry season in October 2017, with a mean low value of  $0.10 \pm 0.003$

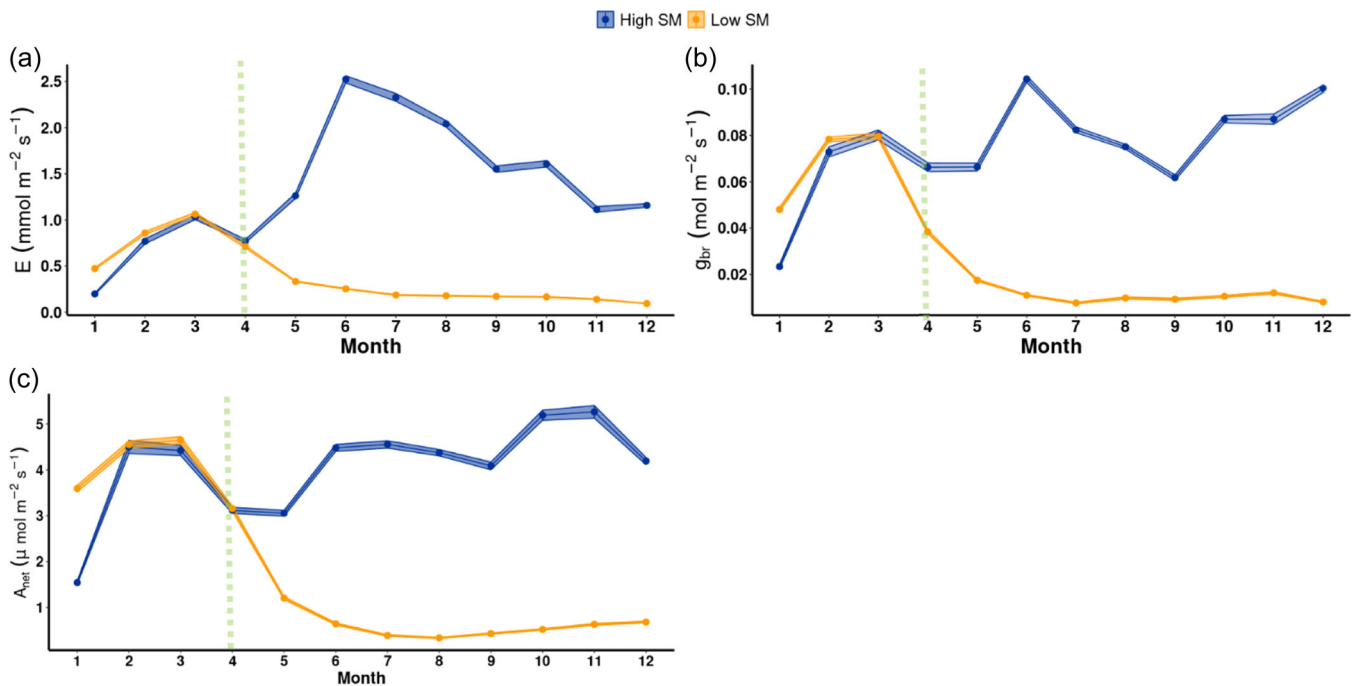


**FIGURE 3** Daytime monthly mean and SE of (a) transpiration ( $E$ ), (b) branch conductance ( $g_{br}$ ), (c) net photosynthesis ( $A_{net}$ ) in the irrigated (blue) and non-irrigated (orange) trees from January to December 2017. The green dotted line represents the irrigation start date in May 2017. SE, standard error; SM, soil moisture. [Color figure can be viewed at [wileyonlinelibrary.com](http://wileyonlinelibrary.com)]

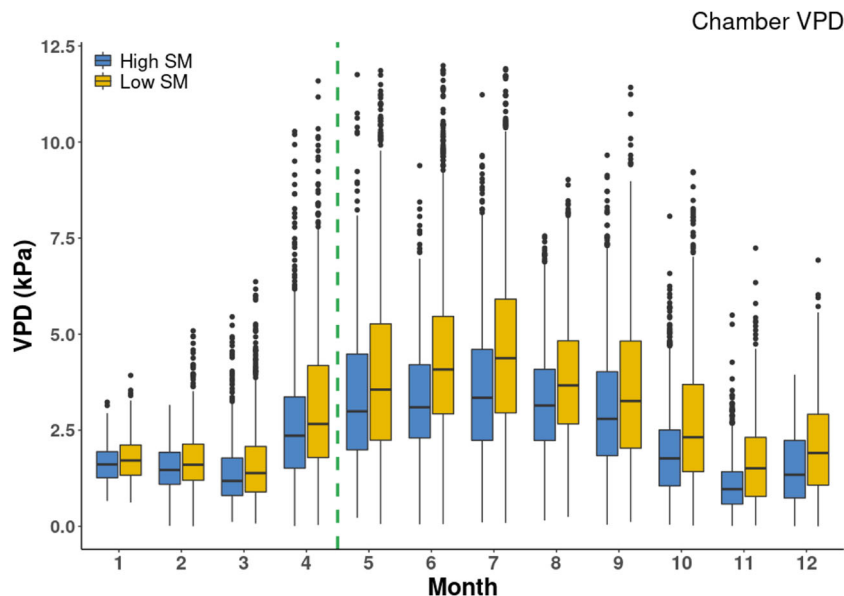


**FIGURE 4** Boxplot of the daytime vapour pressure deficit (VPD) as measured inside the chambers ( $n = 7$  per plot) by month. Each month represents  $1670 \pm 100$  and  $1744 \pm 87$  sampling points for the high-soil moisture (SM) and low-SM trees, respectively. The lower and upper box boundaries represent the 25th and 75th percentiles, respectively, the line inside the box is the median, the lower and upper error lines are the 10th and 90th percentiles, respectively, and the filled circles are data points falling outside 10th and 90th percentiles. Irrigation begun in May 2017 (green dotted line). Occasions of high VPD ( $> 5$  kPa) occurred in both chambers, and the differences between the chambers' mean values before and after irrigation is not significant ( $p > 0.05$ ). [Color figure can be viewed at [wileyonlinelibrary.com](http://wileyonlinelibrary.com)]

between July and October. Hence, a full separation between soil and atmospheric drought was achieved.

The initial physiological response to the onset of irrigation was fast even though it occurred under relatively dry conditions (VPD of 6 kPa and REW of 0.3 on that week).  $E$  increased rapidly, and after 20 days, it reached relatively stable values for the following 2 months (Figure 3a and Supporting Information: Figure S6). Midday  $E$  averaged  $1.8 \pm 0.1 \text{ mol m}^{-2} \text{ s}^{-1}$  at 20 days after irrigation onset, simultaneously being four times the pre-irrigation rates and an order of magnitude higher than the low-SM rates ( $0.2 \pm 0.4 \text{ mol m}^{-2} \text{ s}^{-1}$ ). During the first 20 days of irrigation,  $g_{br}$  increased to  $0.098 \pm 0.002 \text{ mol m}^{-2} \text{ s}^{-1}$  and was maintained at these high levels, ranging between 0.09 and  $0.11 \text{ mol m}^{-2} \text{ s}^{-1}$ . These values were 2.3 times higher than the pre-irrigation values and were over 15 times higher than the mean value ( $0.005 \pm 0.003 \text{ mol m}^{-2} \text{ s}^{-1}$ ) of the low-SM trees during the same period. Midday  $A_{net}$  increased in the high-SM trees and stabilised after approximately 5 days at  $4.2 \pm 0.65 \text{ } \mu\text{mol m}^{-2} \text{ s}^{-1}$ , a level at which it remained stable for the next 60 days, and was approximately two times higher than the pre-irrigation levels and nearly 20 times higher than the  $A_{net}$  values in the low-SM trees during the same period. This fast and strong response of the high-SM trees occurred despite the concomitant sharp increase in VPD from midday mean values of  $2.6 \pm 0.94$  kPa during the pretreatment period to  $4.2 \pm 1.09$  kPa (Figure 4). An exception was the week of the start of the irrigation treatment, when VPD values were above average, between 5 and 6.5 kPa (Supporting Information: Figure S7). For detailed data on days after irrigation, see Supporting Information: Figures S6 and S7.

### 3.3 | Effects of eliminating soil drying on gas exchange

Comparing the wet and dry periods (March and July, peak activity, and peak dry periods in the untreated forest plot) at the tree scale

based on the branch chamber measurements showed that in the high-SM trees,  $E$  increased 2.5 times (Figure 3a),  $g_{br}$  increased 1.2 times (Figure 3b), and  $A_{net}$  remained high and stable throughout the entire dry season (Figure 3c). The total amount of transpiration per ground area calculated from the branch chamber fluxes between May and August was approximately 400 mm in the high-SM plot (while  $\sim 470$  mm of irrigation water was applied) and approximately 32 mm in the low-SM plot based on our site estimates of leaf area index (LAI) of 1.8 and tree density of  $300 \text{ tree ha}^{-1}$ .

In the low-SM trees, the diel dynamics of leaf gas exchange differed markedly between the wet (Nov–Apr) and dry (May–Oct) seasons. During the wet season, a clear diel trend was observed, with  $E$ ,  $g_{br}$ , and  $A_{net}$  starting to increase after sunrise, peaking at midday, and decreasing toward the evening (Figure 5a–c), closely following the photosynthetically active radiation (PAR) and VPD trends. At the start of the dry season, the amplitude of the diel cycles in these parameters decreased, and the daily peak shifted to a distinct early morning peak of  $E$ ,  $g_{br}$ , and  $A_{net}$  followed by a decline in activities throughout the remainder of the day. Notably, the low-SM trees still lost water throughout the day, possibly due to cuticular transpiration, and  $A_{net}$  increased in the late afternoon after recovering from the midday depression.

In the high-SM trees (Figure 5d–f), the diel trend did not change from the wet to the dry seasons. In both seasons, gas exchange was highest during midday, despite the peak in VPD at that time ( $\sim 1.5$  and  $\sim 4.4$  kPa in the wet and dry seasons, respectively; Figure 4 and Supporting Information: Figure S7). In contrast to the low-SM trees, the  $g_{br}$  of the high-SM trees peaked at 10:00 and was maintained at high values throughout the day until 15:00 to 16:00 (Figure 5d), as was also observed for  $E$  and  $A_{net}$  (Figure 5e,f).

One of the more dramatic effects of the supplemented dry season irrigation was the response of  $E$ . The natural atmospheric

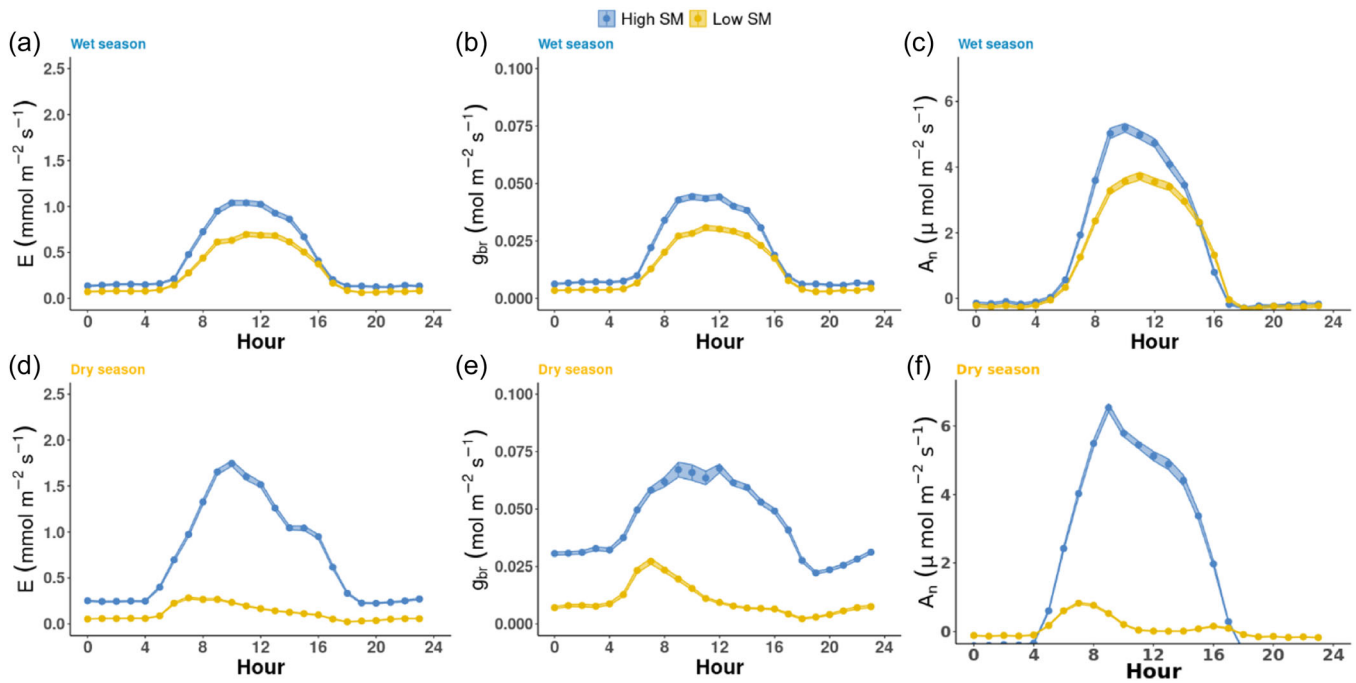


**FIGURE 5** Diel dynamics of the mean daily values of the branch chamber gas exchange measurements at both plots for the wet (a–c) and dry (d–f) seasons. Each data point represents the mean value  $\pm$  SE for 85 days of measurement per season for transpiration (a, d), branch stomatal conductance (b, e), and net photosynthesis (c, f). SE, standard error; SM, soil moisture. [Color figure can be viewed at [wileyonlinelibrary.com](http://wileyonlinelibrary.com)]

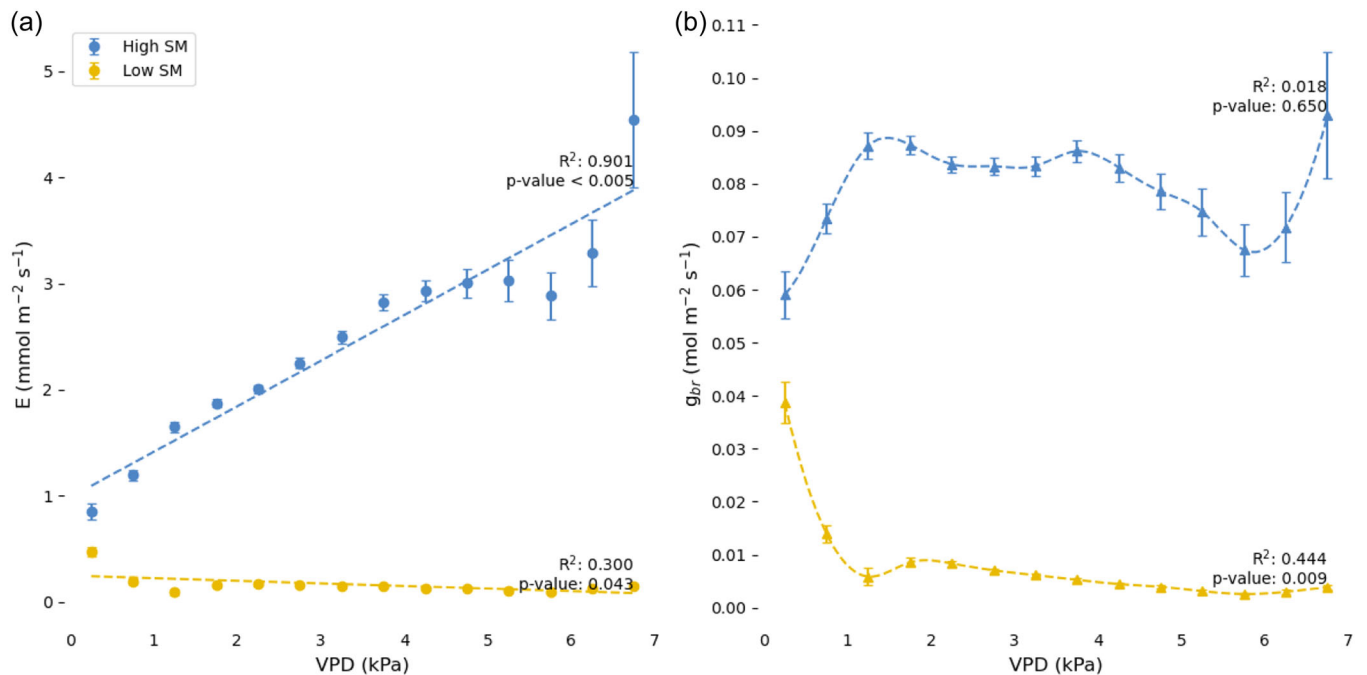


**FIGURE 6** Relationships between daytime  $E$  and vapour pressure deficit (VPD) (a) and  $g_{br}$  and VPD (b) during the dry season (May–Oct). VPD data were binned every 0.5 kPa, and each data point represents all the values of  $E$  and  $g_{br}$  for the corresponding VPD range. Each plot represents an average of 7 trees and  $n > 5000$  for each data point that was binned in the graph. [Color figure can be viewed at [wileyonlinelibrary.com](http://wileyonlinelibrary.com)]

drought (VPD), as measured next to the branch chambers after the irrigation started, ranged from 0.5 kPa to high dry season values of 5.5 kPa. However, the combination of stable water supply across seasons, accompanied by this large seasonal increase in VPD, resulted

in a strong positive relationship between  $E$  and VPD values (Figure 6). This was associated with a mild increase in  $g_{br}$ , which remained relatively high even under extreme VPD values ( $>3.5$  kPa). In contrast, a negative relationship (slope =  $-0.08$ ) between  $E$  and VPD developed

in the low-SM trees (Figure 6), associated with a decrease in  $g_{br}$  from 0.01 to 0.005 mol m<sup>-2</sup> s<sup>-1</sup> as VPD increased above 2 kPa, after the sharp decrease in the low VPD values (0–1 kPa) occurring only in the early morning during the dry season.

### 3.4 | Model simulations of stomatal response

Simulations with the hydraulic model of the response of  $E$  to VPD, both before and after irrigation, showed good agreement with the measurement results. A similar trend with no significant difference ( $p = 0.6–0.9$ ) was found before irrigation (February–April conditions) in both the low-SM and high-SM trees, but clear differences in  $g_{br}$  between treatments ( $p < 0.05$ ) developed after irrigation (June–August) in response to increasing VPD (Figure 7a,b). In both field measurements and model simulations, the  $g_{br}$  in the high-SM trees showed some decline in response to

increasing VPD but remained at high levels even under high VPD values (Figures 6 and 7b).

Similar agreements between measurements and model simulations were observed for the response of  $E$  to changes in VPD, both before and after irrigation was initiated (Figure 7c,d). Here, too, no significant differences in trends ( $p > 0.05$ ) were observed before irrigation between low-SM and high-SM trees, but a clear difference developed after irrigation ( $p < 0.05$ ), as the simulated SM was elevated.

## 4 | DISCUSSION

Using irrigation to eliminate dry season soil drought while atmospheric drought (VPD) reached its seasonal peak enabled us to decouple the effects of the two stressors and assess the differential response of mature pine trees to each of them.

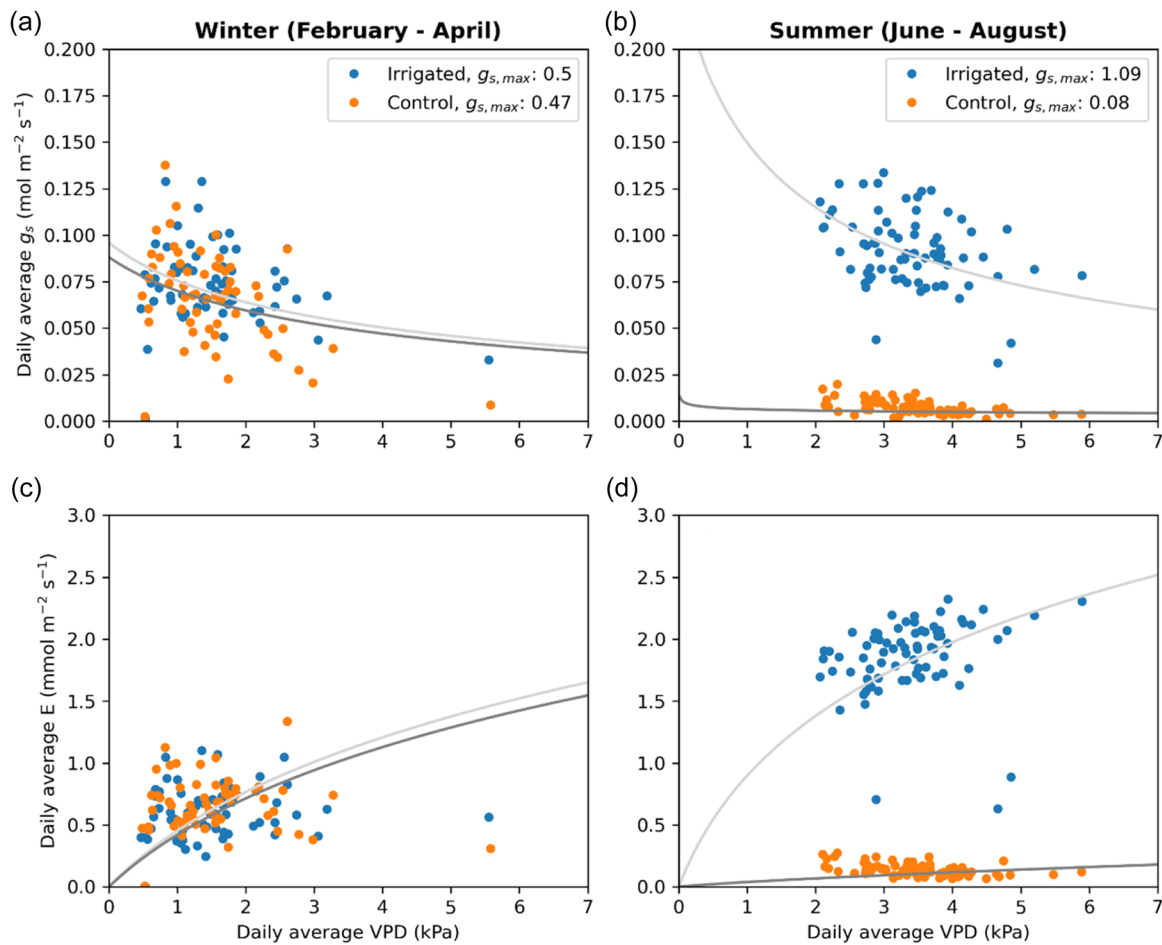


**FIGURE 7** Model output (line) and measurement (dots) results of branch transpiration (a, b) and stomatal conductance (c, d) responses to increasing vapour pressure deficit (VPD) before (a, c) and after (b, d) irrigation. Maximal stomatal conductance ( $g_{s,max}$ ) was determined for each period and each treatment separately and is shown in the legend. Maximal stem hydraulic conductivity ( $k_{x,max}$ ) was set as 0.5 mol/m<sup>2</sup>/s and 2.0 mol/m<sup>2</sup>/s for the winter and summer periods, respectively.  $\Psi_{S,0}$  and  $d\Psi_s$  are the soil water potential values that occurred with the highest and lowest VPD, respectively, in the low-SM area during each period. These values represent the daily range of soil water potential. [Color figure can be viewed at [wileyonlinelibrary.com](http://wileyonlinelibrary.com)]

#### 4.1 | Fast recovery and long-term resilience

The onset of supplemental irrigation in mid-May occurred 3 months after the last rain event. At that time, the soil REW was below 0.3, the VPD was approximately 5–6 kPa (Supporting Information: Figure S7), and the  $E$  and  $A_{net}$  levels approached their seasonal minima. These conditions allowed us to test and demonstrate Aleppo pine tree resilience in semiarid conditions. We showed that irrigation led to a rapid (2–3 days) recovery and restored the prestress gas exchange values. These results suggest that the high-SM trees maintained the wet-season water transport capacity with the existing conductive system. Resilience, defined as the ability to recover from stress while minimising losses in productivity (Ruehr et al., 2019; Tatarinov et al., 2016), is a key trait of mature Aleppo pine trees growing in semiarid environments. It is likely to contribute to their survival in an environment that is characterised by a long dry season and a relatively short and highly variable wet season (Ungar et al., 2013; Wang et al., 2020), as well as a season with a high frequency of heatwave events (Birami et al., 2018a; Tatarinov et al., 2016).

This rapid recovery may also indicate a low rate of native embolism (conduits in an air-filled state (Tyree & Sperry, 1989)) in these trees, supported by previous studies that showed a 50% loss of hydraulic conductivity ( $PLC_{50}$ ) in the range of  $-3.2$  to  $-5$  MPa  $\Psi_{leaf}$  in Aleppo pines (David-Schwartz et al., 2016; Klein et al., 2011; Oliveras et al., 2003). However, at our study site, the lowest measured midday  $\Psi_{leaf}$  in the dry season was approximately  $-3.2$  MPa, further implying nonlethal damage to the hydraulic system (Hammond et al., 2019) due to the redundancy of xylem conduits (Körner, 2019), allowing the trees to operate at narrow hydraulic safety margins (Klein et al., 2011). Interestingly, a recent study by Wagner et al. at the same study site showed a clear link between low rates of needle embolism and high VPD events, while SM did not affect the percent loss of conductivity (Wagner et al., 2022). This may suggest that the stomatal hyposensitivity to high VPD shown in our study could increase the risk of low rates of native embolism. However, according to the low embolism rates found in that study (12%), it appears that soil drought is a more chronic problem related to severe hydraulic damage due to embolism than high VPD.

#### 4.2 | Irrigation changes the peak activity period of $E$ but not $A_{net}$ and $g_{br}$

The peak activity period of the Yatir forest typically occurs in early March, which represents a large difference from the time of peak activity in Northern Hemisphere temperate forests around July (Rotenberg & Yakir, 2010; Wang et al., 2020). Although maximum temperature and radiation are usually attained in July, due to the severely dry soil conditions and high VPD at this site, photosynthesis and transpiration are suppressed by low stomatal conductance (Klein et al., 2014; Preisler et al., 2019). However, using supplemental irrigation to prevent dry season soil drying resulted in a new peak in  $E$  in the high-SM trees during the dry season (Figure 3), with

transpiration rates and VPD values approximately three times higher than during the natural peak in March. This was accompanied by a prominent rise in  $A_{net}$  and  $g_{br}$  with values typical of the nonstress wet season, peaking around July. The results support the idea that the large seasonal shift in peak activity from July in moist regions to March in this dry region is indeed driven by water supply (Park et al., 2019; Wang et al., 2020).

The results also demonstrate that in these trees, stomatal closure in response to high VPD is not a fixed trait (Ball et al., 1987; Grossiord et al., 2020; Novick et al., 2016) but rather dependent on soil water supply and, presumably, on  $\Psi_{leaf}$  (Figure 7). In the absence of soil water limitation, transpiration was clearly driven by VPD, showing a near-linear relationship (Figure 6) that was not accompanied by reduced conductance (Figure 6). This is in contrast to common observations of a reduction in stomatal conductance in response to increasing VPD (Novick et al., 2016). Low-SM trees were the main reason for the decreasing  $g_{br}$  under high VPD, followed by a decrease in  $E$  and  $A_{net}$ , as also shown in other studies (e.g., Lagergren & Lindroth, 2002; Sulman et al., 2016). The sharp decrease in  $g_{br}$  corresponds well to the early morning stomatal behaviour shown in a previous study at this site, as trees are able to use their stored water for early morning transpiration in the dry season (Preisler et al., 2021b).

Our results suggest that being able to exhibit high stomatal conductance under harsh VPD conditions, when soil water is not a limiting factor, is the main reason for the high productivity of Aleppo pine trees in semiarid conditions. Such a VPD–stomata relationship likely underlies the resilience of these trees in stressful environments, such as at our study site, as well as at other sites undergoing climatic changes (Anderegg et al., 2017; Feng et al., 2018; Y. Liu et al., 2020; Wolf et al., 2016).

#### 4.3 | Drivers and limitations of dry season photosynthesis

While  $E$  was shown to be driven by VPD under high SM conditions (Figure 6),  $A_{net}$  was driven by PAR, temperature, and  $[CO_2]$  and not limited by VPD. The relief of soil drought stress in the high-SM trees did not enable higher photosynthetic activity during the hot and dry season despite the considerable improvement in conditions, for example, temperatures in the optimum range ( $26.6^\circ\text{C}$  in July vs.  $16.9^\circ\text{C}$  in March) (Birami et al., 2020; Sage, 2021), ample radiation (PAR at 6 m height in the canopy was  $1800 \mu\text{mol m}^{-2} \text{s}^{-1}$ ), and sufficient water supply. Under these conditions,  $A_{net}$  in the low-SM trees was near zero in July, but in the high-SM trees, it reached values similar to those at the peak annual cycle in March. Why did these rates not increase further under the near-optimal high SM conditions? This may be due to several factors. First, we note that the instantaneous increase in PAR exceeded the light saturation point, which leads to photoinhibition, as was determined in our earlier studies at the same site (Maseyk et al., 2008, 2019). Second, thermal effects in the hot environment could lead to nonstomatal limitations

such as mesophyll conductance and biochemical limitations constraining maximal  $A_{net}$  and plant productivity in the dry season (Gimeno et al., 2019; Salmon et al., 2020). However, note that effective leaf/branch heat dissipation and low  $\Delta T_{leaf-air}$  were extensively demonstrated recently in this experimental system (Muller et al., 2021a). The second reason could be related to other nonstomatal limitations (mesophyll conductance and biochemical limitations) constraining maximal  $A_{net}$  and productivity in the dry season (Salmon et al., 2020).

#### 4.4 | Role of SM and VPD in stomatal regulation

A range of experimental and model studies proposed VPD as the main factor influencing  $g_s$  (e.g., Ball et al., 1987; Buckley, 2005; Grossiord et al., 2020; Medlyn et al., 2011; Novick et al., 2016). However, our results are consistent with recent studies using both hydraulic models and experiments (Fang et al., 2021; Y. Liu et al., 2020; Massmann et al., 2019) that also suggest a greater role of plant water potential and SM than of VPD in regulating stomatal response to drought (Anderegg et al., 2017; Martínez-Vilalta & Garcia-Forner, 2017; L. Liu et al., 2020). Low sensitivity of stomatal conductance to high VPD under sufficient SM was also shown in Aleppo pine seedlings under greenhouse-controlled conditions (Birami et al., 2018b), crop plants (Cohen & Hochberg et al., 2017; Cohen & Naor, 2002; Paudel et al., 2015), *Quercus rotundifolia* (David et al., 2004) and several isohydric trees (Bond et al., 2008), with VPD levels reaching values of 3.5 kPa. Nevertheless, the present study significantly extends the range of the reported responses in a key tree species in the Mediterranean basin to more extreme conditions, reaching ambient VPD levels of 7 kPa.

Maintaining high stomatal conductance in extremely dry air, as in this study, is unusual, but clearly, this is supported by high SM. This may be at least partly in line with some climate change predictions that in drying regions, decreasing precipitation will be associated with increasing storm intensity (Drori et al., 2021). This may or can improve soil water content due to better infiltration and reduced evaporation (Assefa-Haile, 2019), partly offset the drying trends, and mitigate the impact of the concomitant increase in atmospheric VPD.

Some plant traits can result in reduced sensitivity of  $g_s$  to high VPD or mask such a response (McAdam & Brodribb, 2016; McAdam et al., 2011). An example of such a response is the sunken stomata of pine (Howard, 1973), producing microclimate isolation between the dry background atmosphere and the air boundary layer in the stomatal cavity. The significant nighttime transpiration observed in the high-SM trees during the dry season when VPD was  $\geq 1$  kPa (Figure 5d,e) may indicate a minimal  $g_{br}$  or cuticular transpiration for these trees that limits their response to VPD. The slow production of abscisic acid (ABA) in conifers, usually in response to changes in  $\Psi_{leaf}$  that are assumed to remain high in the high-SM tree, may also lead to reduced sensitivity of stomatal conductance to high VPD (McAdam & Brodribb, 2014).

#### 4.5 | Is water potential a better predictor of stomatal conductance than VPD in hydraulic models?

Our results showed good agreement between the branch-scale measurements and the model simulations of stomatal conductance (Figure 7). Specifically, the simple hydraulic model demonstrates the effects of  $\Psi_{leaf}$  on  $g_s$  and  $E$ , which varies based on the  $\Psi_{soil}$  and VPD as the two end-members. The model shows that  $g_s$  is sensitive to  $\Psi_{leaf}$ , which could remain relatively high even under high VPD conditions as long as sufficient SM and high  $\Psi_{leaf}$  are maintained. The combined experimental and model simulation results support the conclusions that (1) SM and atmospheric VPD can have differential effects on leaf gas exchange and (2) SM supply and plant water potential can have a prevailing effect on the sensitivity of stomatal conductance to VPD, even under very high VPD values. Such interactions are not well resolved at present in eco-physiological and Earth system models that forecast vegetation response to climate change since they use VPD as a limiting factor and not as a driving force (Anderegg et al., 2018; Bartlett et al., 2018; Mirfenderesgi et al., 2016; Sperry & Love, 2015; Sperry et al., 2016). It is worth noting that accurately measuring  $\Psi_{soil}$  in very dry soil can be problematic and can lead to unrealistic negative values. Additionally, predawn leaf water potential ( $\Psi_{pD}$ ) does not directly represent  $\Psi_{soil}$ , and only a few models can estimate these values, as described in previous studies (Preisler et al., 2021a; Saxton et al., 1986). The large  $\Delta\Psi_{leaf}$  (predawn and midday) in the high-SM trees ( $\sim 1$  MPa) compared to that of the low-SM trees ( $\sim 0.2$  MPa) during the dry season (Supporting Information: Figure S8) is additional evidence demonstrating that the stomatal response to a decrease in water supply overrode the response to high VPD.

## 5 | CONCLUSIONS

Although this is a 1-year study that should be further extended to reduce uncertainties, it offered a unique combination between extensive field measurements on mature pine trees under extreme environmental conditions and elimination of the dry season soil drought under high atmospheric VPD through experimental manipulation. This setup provided novel insights into the importance hierarchy of soil and atmospheric droughts on the ecophysiology of Aleppo pine trees. The results indicated that VPD is not limiting when its differential increase (i.e., while SM remains high) does not decrease stomatal conductance (presumably due to stem hydraulic conductivity, preventing changes in leaf water potential). This study also highlights the need to quantify the possible mitigating effects of maintaining  $\Psi_{soil}$  on the impact of increasing atmospheric VPD for predicting ecosystem response to climate change.

## ACKNOWLEDGMENTS

The work was partly funded by the German Research Foundation through its German-Israeli project cooperation programme Climate feedbacks and benefits of semiarid forests (CLIFF; grant nos. YA 274/

1-1 and SCHM 2736/2-1), Israel Science Foundation (ISF 1976/17), NSFC-ISF (grant 2579/16), Keren Kayemet Lelsrael (KKL 90-10-012-11), and Ring Family Foundation. The long-term operation of the Yatir Forest Research Field Site is supported by the Cathy Wills and Robert Lewis Programme in Environmental Sciences. The authors thank the United States-Israel Binational Agriculture Research and Development Fund Vaadia-BARD Postdoctoral Fellowship Award no. FI-584-2019. XF was supported by National Science Foundation award DEB-2045610. We thank Andrew Feldman for providing constructive comments on the manuscript and members of our laboratory for valuable discussions and comments on the manuscript. We also thank all the students who helped establish the research operation: Nadav Steinberg, Rachel Sarel, Yonatan Darom, Guy Sadot, Roni Tal, and Sagi Gottlieb. We are grateful to Hagai Sagi, Andreas Gast, Alex Jahanfard, Einan Dafna, and Chaim Madar for their vital and crucial contributions to setup planning, design, and construction.

#### DATA AVAILABILITY STATEMENT

Data for the Yatir field site are publicly available through Fluxnet (<https://fluxnet.org/>), are available in the SI section, or are available from the corresponding authors upon reasonable request.

#### ORCID

Yakir Preisler  <https://orcid.org/0000-0001-5861-8362>

Xue Feng  <http://orcid.org/0000-0003-1381-3118>

Jonathan D. Muller  <https://orcid.org/0000-0003-0475-3897>

#### REFERENCES

- Allen, C.D., Breshears, D.D. & McDowell, N.G. (2015) On underestimation of global vulnerability to tree mortality and forest die-off from hotter drought in the Anthropocene. *Ecosphere*, 6, art129.
- Allen, C.D., Macalady, A.K., Chenchouni, H., Bachelet, D., McDowell, N., Vennetier, M. et al. (2010) A global overview of drought and heat-induced tree mortality reveals emerging climate change risks for forests. *Forest Ecology and Management*, 259, 660–684.
- Alpert, P., Krichak, S.O., Shafir, H., Haim, D. & Osetinsky, I. (2008) Climatic trends to extremes employing regional modeling and statistical interpretation over the E. Mediterranean. *Global and Planetary Change*, 63, 163–170.
- Anderegg, W.R.L., Wolf, A., Arango-Velez, A., Choat, B., Chmura, D.J., Jansen, S. et al. (2017) Plant water potential improves prediction of empirical stomatal models. *PLoS One*, 12, e0185481.
- Anderegg, W.R.L., Wolf, A., Arango-Velez, A., Choat, B., Chmura, D.J., Jansen, S. et al. (2018) Woody plants optimise stomatal behaviour relative to hydraulic risk. *Ecology Letters*, 21, 968–977.
- Assefa-Haile, S. (2019) How does precipitation pattern affect annual tree growth? A multi-year data analysis a case study of semi-arid Yatir Forest, Israel.
- Ault, T.R. (2020) On the essentials of drought in a changing climate. *Science*, 368, 256–260. <https://doi.org/10.1126/science.aaz5492>
- Ball, J.T., Woodrow, I.E. & Berry, J.A. (1987) A model predicting stomatal conductance and its contribution to the control of under different environmental conditions. In: Biggins, J. (Ed.) *Progress in photosynthesis research*. Dordrecht: Springer, pp. 221–224.
- Bamberger, I., Ruehr, N.K., Schmitt, M., Gast, A., Wohlfahrt, G. & Arneth, A. (2017) Isoprene emission and photosynthesis during heat waves and drought in black locust. *Biogeosciences*, 14(15), 3649–3667.
- Bartlett, M.K., Detto, M. & Pacala, S.W. (2018) Predicting shifts in the functional composition of tropical forests under increased drought and CO<sub>2</sub> from trade-offs among plant hydraulic traits. *Ecology Letters*, 22, 67–77.
- Birami, B., Gattmann, M., Heyer, A.G., Grote, R., Arneth, A. & Ruehr, N.K. (2018a) Heat waves alter carbon allocation and increase mortality of Aleppo pine under dry conditions. *Frontiers in Forests and Global Change*, 1, 8.
- Birami, B., Gattmann, M., Heyer, A.G., Grote, R., Arneth, A. & Ruehr, N.K. (2018b) Heat waves alter carbon allocation and increase mortality of Aleppo pine under dry conditions. *Frontiers in Forests and Global Change*, 1, 1–17.
- Birami, B., Nägele, T., Gattmann, M., Preisler, Y., Gast, A., Arneth, A. et al. (2020) Hot drought reduces the effects of elevated CO<sub>2</sub> on tree water-use efficiency and carbon metabolism. *New Phytologist*, 226, 1607–1621.
- Bond, B.J., Meinzer, F.C. & Brooks, J.R. (2008) How trees influence the hydrological cycle in forest ecosystems. In: Wood, P.J. & Hannah, D.M. (Eds.) *Hydroecology and ecohydrology: past, present and future*. USA: John Wiley & Sons, pp. 7–35.
- Breshears, D.D., Adams, H.D., Eamus, D., McDowell, N.G., Law, D.J., Will, R.E. et al. (2013) The critical amplifying role of increasing atmospheric moisture demand on tree mortality and associated regional die-off. *Frontiers in Plant Science*, 4, 266.
- Brodribb, T.J. & Holbrook, N.M. (2003) Stomatal closure during leaf dehydration, correlation with other leaf physiological traits. *Plant Physiology*, 132, 2166–2173.
- Brodribb, T.J., Holbrook, N.M., Edwards, E.J. & Gutiérrez, M.V. (2003) Relations between stomatal closure, leaf turgor and xylem vulnerability in eight tropical dry forest trees. *Plant, Cell & Environment*, 26, 443–450.
- Buckley, T.N. (2005) The control of stomata by water balance. *New Phytologist*, 168, 275–292.
- Burke, E.J., Brown, S.J. & Christidis, N. (2006) Modeling the recent evolution of global drought and projections for the twenty-first century with the Hadley Centre climate model. *Journal of Hydrometeorology*, 7, 1113–1125.
- von Caemmerer, S. & Farquhar, G.D. (1981) Some relationships between the biochemistry of photosynthesis and the gas exchange of leaves. *Planta*, 153, 376–387.
- Choat, B., Jansen, S., Brodribb, T.J., Cochard, H., Delzon, S., Bhaskar, R. et al. (2012) Global convergence in the vulnerability of forests to drought. *Nature*, 491, 752–755.
- Cobb, R.C., Ruthrof, K.X., Breshears, D.D., Lloret, F., Aakala, T., Adams, H.D. et al. (2017) Ecosystem dynamics and management after forest Die-Off: a global synthesis with conceptual state-and-transition models. *Ecosphere*, 8, e02034.
- Cochard, H., Bréda, N. & Granier, A. (1996) Whole tree hydraulic conductance and water loss regulation in *Quercus* during drought: evidence for stomatal control of embolism? *Annales of Forest Sciences*, 53(2–4), 197–206.
- Cohen S. & Naor, A. (2002) The effect of three rootstocks on water use, canopy conductance and hydraulic parameters of apple trees and predicting canopy from hydraulic conductance. *Plant, Cell and Environment*, 25, 17–28.
- Damour, G., Simonneau, T., Cochard, H. & Urban, L. (2010) An overview of models of stomatal conductance at the leaf level. *Plant, Cell and Environment*, 33, 1419–1438.
- David, T.S., Ferreira, M.I., Cohen, S., Pereira, J.S. & David, J.S. (2004) Constraints on transpiration from an evergreen oak tree in Southern Portugal. *Agricultural and Forest Meteorology*, 122, 193–205.
- David-Schwartz, R., Paudel, I., Mizrahi, M., Delzon, S., Cochard, H., Lukyanov, V. et al. (2016) Indirect evidence for genetic differentiation in vulnerability to embolism in *Pinus halepensis*. *Frontiers in Plant Science*, 7, 1–13.

- Dewar, R., Mauranen, A., Mäkelä, A., Hölttä, T., Medlyn, B. & Vesala, T. (2018) New insights into the covariation of stomatal, mesophyll and hydraulic conductances from optimization models incorporating nonstomatal limitations to photosynthesis. *New Phytologist*, 217, 571–585.
- Domec, J.C., Noormets, A., King, J.S., Sun, G., McNulty, S.G. & Gavazzi, M.J. et al. (2009) Decoupling the influence of leaf and root hydraulic conductances on stomatal conductance and its sensitivity to vapour pressure deficit as soil dries in a drained loblolly pine plantation. *Plant, Cell & Environment*, 32, 980–991.
- Dracup, J.A., Lee, K.S. & Paulson, E.G. (1980) On the definition of droughts. *Water Resources Research*, 16, 297–302.
- Drori, R., Ziv, B., Saaroni, H., Etkin, A. & Sheffer, E. (2021) Recent changes in the rain regime over the Mediterranean climate region of Israel. *Climatic Change*, 167, 15.
- Fang, Y., Leung, L.R., Wolfe, B.T., Detto, M., Knox, R.G. & McDowell, N.G. et al. (2021) Disentangling the effects of vapor pressure deficit and soil water availability on canopy conductance in a seasonal tropical forest during the 2015 El Niño drought. *Journal of Geophysical Research: Atmospheres*, 126(10), e2021JD035004.
- Feldman, A.F., Short Gianotti, D.J., Trigo, I.F., Salvucci, G.D. & Entekhabi, D. (2020) Land-atmosphere drivers of landscape-scale plant water content loss. *Under Review in Geophysical Research Letters*, 47(22), e2020GL090.
- Feng, X., Ackerly, D.D., Dawson, T.E., Manzoni, S., Skelton, R.P., Vico, G. et al. (2018) The ecohydrological context of drought and classification of plant responses. *Ecology Letters*, 21, 1723–1736.
- Gimeno, T.E., Saavedra, N., Ogée, J., Medlyn, B.E. & Wingate, L. (2019) A novel optimization approach incorporating non-stomatal limitations predicts stomatal behaviour in species from six plant functional types. *Journal of Experimental Botany*, 70, 1639–1651. <https://academic.oup.com/jxb/article/70/5/1639/5306169>
- Granier, A. (1985) Une nouvelle méthode pour la mesure du flux de sève brute dans le tronc des arbres. *Annales des Sciences Forestières*, 42, 193–200.
- Grossiord, C., Buckley, T.N., Cernusak, L.A., Novick, K.A., Poulter, B. & Siegwolf, R.T.W. et al. (2020) Plant responses to rising vapor pressure deficit. *New Phytologist*, 226, 1550–1566.
- Grossiord, C., Sevanto, S., Borrego, I., Chan, A.M., Collins, A.D., Dickman, L.T. et al. (2017) Tree water dynamics in a drying and warming world. *Plant, Cell & Environment*, 40, 1861–1873.
- Grünzweig, J.M., Lin, T., Rotenberg, E., Schwartz, A. & Yakir, D. (2003) Carbon sequestration in arid-land forest. *Global Change Biology*, 9, 791–799.
- Hammond, W.M., Williams, A.P., Abatzoglou, J.T., Adams, H.D., Klein, T. & López, R. et al. (2022) Global field observations of tree die-off reveal hotter-drought fingerprint for earth's forests. *Nature Communications*, 13, 1761.
- Hammond, W.M., Yu, K., Wilson, L.A., Will, R.E., Anderegg, W.R.L. & Adams, H.D. (2019) Dead or dying? quantifying the point of no return from hydraulic failure in drought-induced tree mortality. *New Phytologist*, 223, 1834–1843.
- Hartmann, H., Bastos, A., Das, A.J., Esquivel-Muelbert, A., Hammond, W.M. & Martínez-Vilalta, J. et al. (2022) Climate change risks to global forest health: emergence of unexpected events of elevated tree mortality worldwide. *Annual Reviews*, 73, 673–702.
- Haworth, M., Elliott-Kingston, C. & McElwain, J.C. (2011) Stomatal control as a driver of plant evolution. *Journal of Experimental Botany*, 62, 2419–2423.
- Hochberg, U., Herrera, J.C., Degu, A., Castellarin, S.D., Peterlunger, E., Alberti, G. et al. (2017) Evaporative demand determines the relative transpirational sensitivity of deficit-irrigated grapevines. *Irrigation Science*, 35, 1–9.
- Howard, E.T. (1973) Properties of southern pine needles. *Wood Science*, 5(4), 281–286.
- IPCC (2018) IPCC 2018 Report: global warming report: global warming of 1.5°C. Chapter I, (pp. 49–91).
- Masson-Delmotte, V., Zhai, P., Pirani, A., Connors, S.L., Péan, C. & Berger, S. (2021) IPCC Climate change 2021: the physical science basis, *Contribution of Working Group I to the Sixth Assessment Report of the Intergovernmental Panel on Climate Change*. Bonn, Germany: IPCC.
- Jarvis, P.G. (1976) The interpretation of the variations in leaf water potential and stomatal conductance found in canopies in the field. *Philosophical Transactions of the Royal Society*, 273, 593–610.
- Klein, T., Cohen, S. & Yakir, D. (2011) Hydraulic adjustments underlying drought resistance of *Pinus halepensis*. *Tree Physiology*, 31, 637–648.
- Klein, T., Rotenberg, E., Cohen-Hilaleh, E., Raz-Yaseef, N., Tatarinov, F., Preisler, Y. et al. (2014) Quantifying transpirable soil water and its relations to tree water use dynamics in a water-limited pine forest. *Ecohydrology*, 7, 409–419.
- Körner, C. (2019) No need for pipes when the well is dry—a comment on hydraulic failure in trees. *Tree Physiology*, 39, 695–700.
- Lagergren, F. & Lindroth, A. (2002) Transpiration response to soil moisture in pine and spruce trees in Sweden. *Agricultural and Forest Meteorology*, 112, 67–85.
- Lange, O.L., Lösch, R., Schulze, E.-D. & Kappen, L. (1971) Responses of stomata to changes in humidity. *Planta*, 100, 76–86.
- Liu, L., Gudmundsson, L., Hauser, M., Qin, D., Li, S. & Seneviratne, S.I. (2020) Soil moisture dominates dryness stress on ecosystem production globally. *Nature Communications*, 11, 1–9.
- Liu, Y., Kumar, M., Katul, G.G., Feng, X. & Konings, A.G. (2020) Plant hydraulics accentuates the effect of atmospheric moisture stress on transpiration. *Nature Climate Change*, 10, 691–695.
- Lloyd-Hughes, B. (2014) The impracticality of a universal drought definition. *Theoretical and Applied Climatology*, 117, 607–611.
- Martínez-Vilalta, J. & García-Forner, N. (2017) Water potential regulation, stomatal behavior and hydraulic transport under drought: deconstructing the iso/anisohydric concept. *Plant, Cell & Environment*, 40, 962–976.
- Maseyk, K., Lin, T., Cochavi, A., Schwartz, A. & Yakir, D. (2019) Quantification of leaf-scale light energy allocation and photoprotection processes in a Mediterranean pine forest under extensive seasonal drought. *Tree Physiology*, 39, 1767–1782.
- Maseyk, K.S., Lin, T., Rotenberg, E., Grünzweig, J.M., Schwartz, A. & Yakir, D. (2008) Physiology-phenology interactions in a productive semi-arid pine forest. *New Phytologist*, 178, 603–616.
- Massmann, A., Gentine, P. & Lin, C. (2019) When does vapor pressure deficit drive or reduce evapotranspiration? *Journal of Advances in Modeling Earth Systems*, 11, 3305–3320.
- McAdam, S.A.M. & Brodribb, T.J. (2012) Fern and lycophyte guard cells do not respond to endogenous abscisic acid. *The Plant Cell*, 24, 1510–1521.
- McAdam, S.A.M. & Brodribb, T.J. (2014) Separating active and passive influences on stomatal control of transpiration. *Plant Physiology*, 164, 1578–1586.
- McAdam, S.A.M. & Brodribb, T.J. (2016) Linking turgor with ABA biosynthesis: implications for stomatal responses to vapor pressure deficit across land plants. *Plant Physiology*, 171, 2008–2016.
- McAdam, S.A.M., Brodribb, T.J., Ross, J.J. & Jordan, G.J. (2011) Augmentation of abscisic acid (ABA) levels by drought does not induce short-term stomatal sensitivity to CO<sub>2</sub> in two divergent conifer species. *Journal of Experimental Botany*, 62, 195–203.
- Medlyn, B.E., Duursma, R.A., Eamus, D., Ellsworth, D.S., Prentice, I.C., Barton, C.V.M. et al. (2011) Reconciling the optimal and empirical approaches to modelling stomatal conductance. *Global Change Biology*, 17, 2134–2144.
- Medlyn, B.E., De Kauwe, M.G., Lin, Y.S., Knauer, J., Duursma, R.A., Williams, C.A. et al. (2017) How do leaf and ecosystem measures of water-use efficiency compare? *New Phytologist*, 216, 758–770.

- Meinzer, F.C., Johnson, D.M., Lachenbruch, B., McCulloh, K.A. & Woodruff, D.R. (2009) Xylem hydraulic safety margins in woody plants: coordination of stomatal control of xylem tension with hydraulic capacitance. *Functional Ecology*, 23, 922–930.
- Mirfenderesgi, G., Bohrer, G., Matheny, A.M., Fatichi, S., de Moraes Frasson, R.P. & Schäfer, K.V.R. (2016) Tree level hydrodynamic approach for resolving aboveground water storage and stomatal conductance and modeling the effects of tree hydraulic strategy. *Journal of Geophysical Research: Biogeosciences*, 121, 1792–1813.
- Muller, J.D. & Oz, I. (2021) Branch-chamber-fluxes; GitHub.
- Muller, J.D., Rotenberg, E., Tatarinov, F., Oz, I. & Yakir, D. (2021a) Evidence for efficient nonevaporative leaf-to-air heat dissipation in a pine forest under drought conditions. *New Phytologist*, 232, 2254–2266.
- Muller, J.D., Rotenberg, E., Tatarinov, F., Vishnevetsky, I., Dingjan, T., Kribus, A. et al. (2021b) 'Dual-reference' method for high-precision infrared measurement of leaf surface temperature under field conditions. *New Phytologist*, 232, 2535–2546.
- Novick, K.A., Ficklin, D.L., Stoy, P.C., Williams, C.A., Bohrer, G., Oishi, A.C. et al. (2016) The increasing importance of atmospheric demand for ecosystem water and carbon fluxes. *Nature Climate Change*, 6, 1023–1027.
- Oliveras, I., Martínez-Vilalta, J., Jimenez-Ortiz, T., José Lledó, M., Escarré, A. & Piñol, J. (2003) Hydraulic properties of *Pinus halepensis*, *Pinus pinea* and *Tetraclinis articulata* in a dune ecosystem of eastern Spain. *Plant Ecology*, 169, 131–141.
- Oren, R., Sperry, J.S., Katul, G.G., Pataki, D.E., Ewers, B.E., Phillips, N. et al. (1999) Survey and synthesis of intra- and interspecific variation in stomatal sensitivity to vapour pressure deficit. *Plant, Cell & Environment*, 22, 1515–1526.
- Oz, I. (2021) *Resilience of Aleppo pine trees to drought and heat as a function of the duration of the stress period during the dry season*. Italy: The Hebrew University of Jerusalem.
- Pammenter, N.W. & Van der Willigen, C. (1998) A mathematical and statistical analysis of the curves illustrating vulnerability of xylem to cavitation. *Tree Physiology*, 18, 589–593.
- Park, T., Chen, C., Macias-Fauria, M., Tømmervik, H., Choi, S., Winkler, A. et al. (2019) Changes in timing of seasonal peak photosynthetic activity in northern ecosystems. *Global Change Biology*, 25(7), 2382–2395. [https://onlinelibrary.wiley.com/doi/full/10.1111/gcb.14638?casa\\_token=TSpvGFRMtfkAAAAA%3AqGt164nxXf2eO9FGyRcgTnB\\_yo9nj7X-s3us6FTifUSIQGO2\\_cBLxZhCv9jyYd-wVAVoYEKQ5PI6inw](https://onlinelibrary.wiley.com/doi/full/10.1111/gcb.14638?casa_token=TSpvGFRMtfkAAAAA%3AqGt164nxXf2eO9FGyRcgTnB_yo9nj7X-s3us6FTifUSIQGO2_cBLxZhCv9jyYd-wVAVoYEKQ5PI6inw)
- Park Williams, A., Allen, C.D., Macalady, A.K., Griffin, D., Woodhouse, C.A., Meko, D.M. et al. (2013) Temperature as a potent driver of regional forest drought stress and tree mortality. *Nature Climate Change*, 3, 292–297.
- Paudel, I., Naor, A., Gal, Y. & Cohen, S. (2015) Simulating nectarine tree transpiration and dynamic water storage from responses of leaf conductance to light and sap flow to stem water potential and vapor pressure deficit. *Tree Physiology*, 35, 425–438.
- Preisler, Y., Hölttä, T., Grünzweig, J.M., Oz, I., Tatarinov, F. & Ruehr, N.K. et al. (2021) The importance of tree internal water storage under drought conditions. *Tree Physiology*, 42(4), 771–783.
- Preisler, Y., Tatarinov, F., Grünzweig, J.M., Bert, D., Ogée, J., Wingate, L. et al. (2019) Mortality versus survival in drought-affected Aleppo pine forest depends on the extent of rock cover and soil stoniness. *Functional Ecology*, 33, 901–912.
- Preisler, Y., Tatarinov, F., Grünzweig, J.M. & Yakir, D. (2021) Seeking the 'point of no return' in the sequence of events leading to mortality of mature trees. *Plant, Cell & Environment*, 41, 1315–1328.
- Pumpanen, J.S., Heinonsalo, J., Rasilo, T., Hurme, K.R. & Ilvesniemi, H. (2009) Carbon balance and allocation of assimilated CO<sub>2</sub> in Scots pine, Norway spruce, and silver birch seedlings determined with gas exchange measurements and 14C pulse labelling. *Trees*, 23, 611–621.
- Rigden, A.J., Mueller, N.D., Holbrook, N.M., Pillai, N. & Huybers, P. (2020) Combined influence of soil moisture and atmospheric evaporative demand is important for accurately predicting US maize yields. *Nature Food*, 1, 127–133.
- Ross, P.J. & Bristow, K.L. (1990) Simulating water movement in layered and gradational soils using the kirchhoff transform. *Soil Science Society of America Journal*, 54, 1519–1524.
- Rotenberg, E. & Yakir, D. (2010) Contribution of semi-arid forests to the climate system. *Science*, 327, 451–454.
- Rotenberg, E. & Yakir, D. (2011) Distinct patterns of changes in surface energy budget associated with forestation in the semiarid region. *Global Change Biology*, 17, 1536–1548.
- Ruehr, N.K., Grote, R., Mayr, S. & Arneith, A. (2019) Beyond the extreme: Recovery of carbon and water relations in woody plants following heat and drought stress. *Tree Physiology*, 39(8), 1285–1299. <https://academic.oup.com/treephys/article/39/8/1285/5423350>
- Ruehr, N.K., Martin, J.G. & Law, B.E. (2012) Effects of water availability on carbon and water exchange in a young ponderosa pine forest: above- and belowground responses. *Agricultural and Forest Meteorology*, 164, 136–148.
- Sage, R.F. (2021) Russ Monson and the evolution of C4 photosynthesis. *Oecologia*, 197, 823–840.
- Salmon, Y., Lintunen, A., Dayet, A., Chan, T., Dewar, R., Vesala, T. et al. (2020) Leaf carbon and water status control stomatal and nonstomatal limitations of photosynthesis in trees. *New Phytologist*, 226, 690–703. <https://nph.onlinelibrary.wiley.com/doi/full/10.1111/nph.16436>
- Saxton, K.E., Rawls, W.J., Romberger, J.S. & Papendick, R.I. (1986) Estimating generalized soil-water characteristics from texture. *Soil Science Society of America Journal*, 50, 1031–1036.
- Sperry, J.S. (2000) Hydraulic constraints on plant gas exchange. *Agricultural and Forest Meteorology*, 104, 13–23.
- Sperry, J.S., Adler, F.R., Campbell, G.S. & Comstock, J.P. (1998) Limitation of plant water use by rhizosphere and xylem conductance: results from a model. *Plant, Cell and Environment*, 21, 347–359.
- Sperry, J.S. & Love, D.M. (2015) What plant hydraulics can tell us about responses to climate-change droughts. *New Phytologist*, 207, 14–27.
- Sperry, J.S., Wang, Y., Wolfe, B.T., Mackay, D.S., Anderegg, W.R.L., McDowell, N.G. et al. (2016) Pragmatic hydraulic theory predicts stomatal responses to climatic water deficits. *New Phytologist*, 212, 577–589.
- Stocker, B.D., Zscheischler, J., Keenan, T.F., Prentice, I.C., Peñuelas, J. & Seneviratne, S.I. (2018) Quantifying soil moisture impacts on light use efficiency across biomes. *New Phytologist*, 218, 1430–1449.
- Sulman, B.N., Roman, D.T., Yi, K., Wang, L., Phillips, R.P. & Novick, K.A. (2016) High atmospheric demand for water can limit forest carbon uptake and transpiration as severely as dry soil. *Geophysical Research Letters*, 43, 9686–9695.
- Tatarinov, F., Rotenberg, E., Maseyk, K., Ogée, J., Klein, T. & Yakir, D. (2016) Resilience to seasonal heat wave episodes in a Mediterranean pine forest. *New Phytologist*, 210, 485–496.
- Tate, E.L. & Gustard, A. (2000) Drought definition: a hydrological perspective. In: Vogt, J.V. & Somma, F. (Eds.) *Drought and drought mitigation in Europe*. Dordrecht, Netherlands: Springer, pp. 23–48.
- Tyree, M.T. & Sperry, J.S. (1988) Do woody plants operate near the point of catastrophic xylem dysfunction caused by dynamic water stress? answers from a model. *Plant Physiology*, 88, 574–580.
- Tyree, M.T. & Sperry, J.S. (1989) Cavitation and embolism. *Water*, 1, 19–38.
- Ungar, E.D., Rotenberg, E., Raz-Yaseef, N., Cohen, S., Yakir, D. & Schiller, G. (2013) Transpiration and annual water balance of Aleppo pine in a semiarid region: implications for forest management. *Forest Ecology and Management*, 298, 39–51.
- Wagner, Y., Feng, F., Yakir, D., Klein, T. & Hochberg, U. (2022) In situ, direct observation of seasonal embolism dynamics in aleppo pine

trees growing on the dry edge of their distribution. *New Phytologist*, 235, 1344–1350.

- Wang, H., Gitelson, A., Sprintsin, M., Rotenberg, E. & Yakir, D. (2020) Ecophysiological adjustments of a pine forest to enhance early spring activity in hot and dry climate. *Environmental Research Letters*, 15, 114054.
- Wolf, A., Anderegg, W.R.L. & Pacala, S.W. (2016) Optimal stomatal behavior with competition for water and risk of hydraulic impairment. *Proceedings of the National Academy of Sciences*, 15(11), E7222–E7230. <https://iopscience.iop.org/article/10.1088/1748-9326/abc2f9/meta>
- Woodruff, D.R., Meinzer, F.C. & Lachenbruch, B. (2008) Height-related trends in leaf xylem anatomy and shoot hydraulic characteristics in a tall conifer: safety versus efficiency in water transport. *New Phytologist*, 180, 90–99.

## SUPPORTING INFORMATION

Additional supporting information can be found online in the Supporting Information section at the end of this article.

**How to cite this article:** Preisler, Y., Grünzweig, J.M., Ahiman, O., Amer, M., Oz, I., Feng, X. et al. (2023) Vapour pressure deficit was not a primary limiting factor for gas exchange in an irrigated, mature dryland Aleppo pine forest. *Plant, Cell & Environment*, 1–16. <https://doi.org/10.1111/pce.14712>